

ON THE ORIENTATION OF ELLIPSOIDAL PARTICLES IN TURBULENT SHEAR FLOW

Pål H. Mortensen & Helge I. Andersson
Department of Energy and Process Engineering,
Norwegian University of Science and Technology
Kolbjørn Hejes v 2 , 7491 Trondheim, Norway
paal.h.mortensen@ntnu.no

Jurriaan J. J. Gillissen & B. J. Boersma
Laboratory for Aero and Hydrodynamics,
Delft University of Technology
Leeghwaterstraat 21 , 2628 CA Delft, The Netherlands

ABSTRACT

Direct numerical simulation (DNS) of small prolate ellipsoidal particles suspended in a turbulent channel flow is reported. The coupling between the fluid and the particles is one-way. The particles are subjected to the hydrodynamic drag force and torque valid for creeping flow conditions. Six different particle cases with varying particle aspect ratios and equivalent response times are investigated. Results show that, in the near-wall region, ellipsoidal particles tend to align with the mean flow direction, and the alignment increases with increasing particle aspect ratio. When the particle inertia increases, the particles are less oriented in the spanwise direction and more oriented in the wall-normal direction. In the core region of the channel, the orientation becomes isotropic.

INTRODUCTION

The suspension of small elongated particles in a turbulent stream occurs in several industrial applications and environmental phenomena. Most of the research on particulate flows consider spherical particles. This is often due to the isotropic nature of the sphere which makes it much easier to consider both mathematically and numerically. Since a sphere is isotropic, its orientation is immaterial, and the translational motion can be solved independently of the rotational motion. On the other hand, for elongated particles the orientation must be considered since it influences the translational motion.

Even though most of the literature considers spherical particles (see for instance Marchioli et al. (2007), Kuerten (2006), Kulick et al. (1994)), the study of elongated particles immersed in a viscous fluid has been a subject for research through several decades. There exist several analytical studies on elongated (ellipsoidal) particles, see for instance Jeffery (1922), Brenner (1963,1964) and Harper and Chang (1968). Also, the literature reports both numerical and experimental work on elongated particle or fiber suspensions, such as Fan and Ahmadi (1995), Zhang et al. (2001), Lin et al. (2003) and Parsheh et al. (2005) to name a few.

The purpose of the present paper is to study how small inertial prolate ellipsoids orient in a turbulent shear flow. The effects of aspect ratio and particle inertia will be reported. It is assumed that the particles are smaller than the inner scales of turbulence for a frictional Reynolds number of 360. Further it is assumed that the flow field in the im-

mediate neighborhood of the particles is locally Stokesian. The ellipsoids are subjected to hydrodynamic drag force and torque (Jeffery (1922)). The coupling between the particles and fluid is one-way, i.e., the flow field only act on the particles.

EULERIAN FLUID DYNAMICS

The incompressible, isothermal and Newtonian fluid into which the particles are released is governed by the continuity and the Navier-Stokes equation

$$\nabla \cdot \mathbf{u} = 0, \quad (1)$$

$$\frac{\partial \mathbf{u}}{\partial t} + \mathbf{u} \nabla \mathbf{u} = \nabla p + Re_*^{-1} \nabla^2 \mathbf{u}. \quad (2)$$

In the equations above, $\mathbf{u} = \langle u_x, u_y, u_z \rangle$ is the fluid velocity vector, p is the pressure and $Re_* = u_* h / \nu$ is the frictional Reynolds number based upon the friction velocity u_* , channel height h and kinematic viscosity ν .

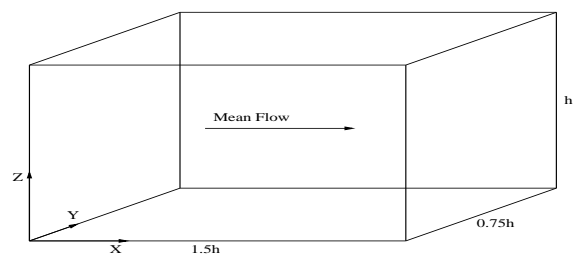


Figure 1: Computational domain.

A direct numerical simulation is used to solve the fluid equations of motion (Eq. (1) and (2)) at a frictional Reynolds number $Re_* = 360$. The size of the computational domain (fig. 1) is $1.5h$ in the streamwise direction, $0.75h$ in the spanwise direction and h in the wall-normal direction. Periodic boundary conditions are applied in the streamwise (x) and spanwise (y) directions, respectively. In the wall-normal direction (z), no-slip conditions are enforced at both walls ($z = 0$ and $z = h$). The computations are carried out with $48 \times 48 \times 192$ gridpoints in the x , y and z directions, respectively. The timestep is $\Delta t^+ = 0.036$ in wall-units. The same algorithm as that used by Gillissen et al. (2007) is employed for solving the fluid equations of motion.

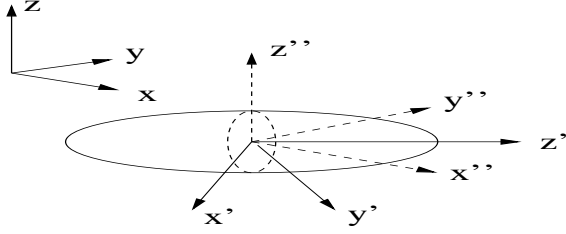


Figure 2: Cartesian coordinate systems; inertial frame \mathbf{x} , particle frame \mathbf{x}' and co-moving frame \mathbf{x}'' .

LAGRANGIAN PARTICLE DYNAMICS

In order to describe the general motion of prolate ellipsoids it is convenient to invoke three different Cartesian coordinate systems: the inertial frame, the particle frame and the co-moving frame. The inertial frame, $\mathbf{x} = \langle x, y, z \rangle$, is the frame that spans the computational domain. The particle frame, $\mathbf{x}' = \langle x', y', z' \rangle$, is attached to the particle with origin at the particle mass-center. The coordinate axes are aligned with the principal directions of inertia. The co-moving frame, $\mathbf{x}'' = \langle x'', y'', z'' \rangle$, is attached to the particle with origin at the mass-center of the particle. The coordinate axes are parallel to the inertial frame. The different coordinate systems are shown in figure 2. The purpose of introducing the co-moving system is to describe the orientational behavior of the ellipsoids. The particle orientation is important since it influences both the rotational and translational motion. The orientation of the particle frame relative to the co-moving frame is given by the the nine direction cosines (Goldstein (1980)) which relates the same vector in two different coordinate systems through the linear transformation $\mathbf{x}' = \mathbf{A}\mathbf{x}''$. The orthogonal transformation matrix \mathbf{A} comprises the direction cosines and is given by

$$\mathbf{A} = \begin{pmatrix} a_{11} & a_{12} & a_{13} \\ a_{21} & a_{22} & a_{23} \\ a_{31} & a_{32} & a_{33} \end{pmatrix} \quad (3)$$

where the direction cosines a_{ij} are

$$\begin{aligned} a_{11} &= e_0^2 + e_1^2 - e_2^2 - e_3^2 \\ a_{12} &= 2(e_1e_2 + e_0e_3) \\ a_{13} &= 2(e_1e_3 - e_0e_2) \\ a_{21} &= 2(e_1e_2 - e_0e_3) \\ a_{22} &= e_0^2 - e_1^2 + e_2^2 - e_3^2 \\ a_{23} &= 2(e_2e_3 + e_0e_1) \\ a_{31} &= 2(e_1e_3 + e_0e_2) \\ a_{32} &= 2(e_2e_3 - e_0e_1) \\ a_{33} &= e_0^2 - e_1^2 - e_2^2 + e_3^2. \end{aligned}$$

The parameters e_0 , e_1 , e_2 and e_3 are the Euler parameters. These parameters are dependent and must satisfy the following constraint

$$e_0^2 + e_1^2 + e_2^2 + e_3^2 = 1. \quad (4)$$

The translational equation of motion is given by the linear momentum relation according to

$$m \frac{d\mathbf{v}}{dt} = \mathbf{F}. \quad (5)$$

Here, m is mass of the ellipsoid and $\mathbf{v} = \langle v_x, v_y, v_z \rangle$ is the velocity vector. The drag force \mathbf{F} , acting on an ellipsoid

under creeping flow conditions is given by (Brenner (1964))

$$\mathbf{F} = \mu \mathbf{A}^t \mathbf{K}' \mathbf{A} (\mathbf{u} - \mathbf{v}) \quad (6)$$

where $\mu = \rho\nu$ is the dynamic viscosity of the fluid. For an ellipse of revolution about the z' -axis, the resistance tensor \mathbf{K}' is

$$\mathbf{K}' = \begin{pmatrix} k'_{xx} & 0 & 0 \\ 0 & k'_{yy} & 0 \\ 0 & 0 & k'_{zz} \end{pmatrix} \quad (7)$$

where k'_{xx} , k'_{yy} , k'_{zz} are the components along the x' , y' , z' axes (principal directions), respectively, and are given as (Gallily and Cohen (1978))

$$k'_{xx} = k'_{yy} = \frac{16\pi a(\lambda^2 - 1)^{\frac{3}{2}}}{(2\lambda - 3) \ln(\lambda + (\lambda^2 - 1)^{\frac{1}{2}}) + \lambda(\lambda^2 - 1)^{\frac{1}{2}}}, \quad (8)$$

$$k'_{zz} = \frac{8\pi a(\lambda^2 - 1)^{\frac{3}{2}}}{(2\lambda - 1) \ln(\lambda + (\lambda^2 - 1)^{\frac{1}{2}}) + \lambda(\lambda^2 - 1)^{\frac{1}{2}}}. \quad (9)$$

In eq. (8) and (9), the aspect ratio $\lambda = b/a$ where a is the semi-minor axis and b is the semi-major axis of the ellipsoid. The particle translational displacement is given by

$$\mathbf{x} = \int \mathbf{v} dt. \quad (10)$$

An important parameter is the particle response time, i.e. the time the particle needs to respond to changes in the flow field due to its inertia. For an ellipsoidal particle which is non-isotropic, the response time is not as obvious as for a spherical particle. Shapiro and Goldenberg (1993) defined an equivalent response time based upon isotropic particle orientation and the inverse of the resistance tensor. Zhang et al. (2001) presented their result in the form

$$\tau^+ = \frac{2\lambda Da^{+2} \ln(\lambda + \sqrt{\lambda^2 - 1})}{9 \sqrt{\lambda^2 - 1}} \quad (11)$$

where D is the density ratio of particle to fluid. The superscript “+” indicates that the parameters are scaled with viscous units ν and u_* .

The rotational motion of the ellipsoids is given by the Euler equations (Goldstein (1980))

$$I'_{xx} \frac{d\omega'_x}{dt} - \omega'_y \omega'_z (I'_{yy} - I'_{zz}) = N'_x \quad (12)$$

$$I'_{yy} \frac{d\omega'_y}{dt} - \omega'_z \omega'_x (I'_{zz} - I'_{xx}) = N'_y \quad (13)$$

$$I'_{zz} \frac{d\omega'_z}{dt} - \omega'_x \omega'_y (I'_{xx} - I'_{yy}) = N'_z, \quad (14)$$

where ω'_x , ω'_y and ω'_z are the components of the angular velocity vector, respectively. Notice that the Euler equations are solved in the particle frame. The principal moments of inertia are

$$I'_{xx} = I'_{yy} = \frac{(1 + \lambda^2)ma^2}{5}, \quad I'_{zz} = \frac{2ma^2}{5}. \quad (15)$$

The torque components (N'_x , N'_y , N'_z) were derived by Jeffery (1922) for an ellipsoid subjected to linear shear under creeping flow conditions and are given as

$$N'_x = \frac{16\pi\mu a^3 \lambda}{3(\beta_0 + \lambda^2 \gamma_0)} [(1 - \lambda^2)f' + (1 - \lambda^2)(\xi' - \omega'_x)] \quad (16)$$

$$N'_y = \frac{16\pi\mu a^3 \lambda}{3(\lambda^2 \gamma_0 + \alpha_0)} [(\lambda^2 - 1)g' + (\lambda^2 + 1)(\eta' - \omega'_y)] \quad (17)$$

$$N'_z = \frac{32\pi\mu a^3 \lambda}{3(\alpha_0 + \beta_0)} (\chi' - \omega'_z), \quad (18)$$

Table 1: Particle parameters for the six different cases.

Case	λ	D	τ^+	N
F10	10	23	0.5	20000
F30	30	152	0.5	20000
F50	50	377	0.5	20000
S10	10	463	10	20000
S30	30	3052	10	20000
S50	50	7539	10	20000

where f' and g' are the rate of strain coefficients

$$f = \frac{1}{2}(u'_{z,y} + u'_{y,z}) \quad (19)$$

$$g = \frac{1}{2}(u'_{x,z} + u'_{z,x}) \quad (20)$$

and ξ' , η' , χ' are the rotation rate coefficients

$$\xi' = \frac{1}{2}(u'_{z,y} - u'_{y,z}) \quad (21)$$

$$\eta' = \frac{1}{2}(u'_{x,z} - u'_{z,x}) \quad (22)$$

$$\chi' = \frac{1}{2}(u'_{x,y} - u'_{y,x}) \quad (23)$$

The parameters α_0 , β_0 , γ_0 are (Gallily and Cohen (1979))

$$\alpha_0 = \beta_0 = \frac{2\lambda^2(\lambda^2 - 1)^{\frac{1}{2}} + \lambda \ln\left(\frac{\lambda - (\lambda^2 - 1)^{\frac{1}{2}}}{\lambda + (\lambda^2 - 1)^{\frac{1}{2}}}\right)}{2(\lambda^2 - 1)^{\frac{3}{2}}} \quad (24)$$

$$\gamma_0 = \frac{2(\lambda^2 - 1)^{\frac{1}{2}} + \lambda \ln\left(\frac{\lambda - (\lambda^2 - 1)^{\frac{1}{2}}}{\lambda + (\lambda^2 - 1)^{\frac{1}{2}}}\right)}{(\lambda^2 - 1)^{\frac{3}{2}}} \quad (25)$$

The time rate of change of the Euler parameters is related to the particle angular velocities and is given as

$$\begin{pmatrix} \dot{e}_0 \\ \dot{e}_1 \\ \dot{e}_2 \\ \dot{e}_3 \end{pmatrix} = \frac{1}{2} \begin{pmatrix} e_0 & -e_1 & -e_2 & -e_3 \\ e_1 & e_0 & -e_3 & e_2 \\ e_2 & e_3 & e_0 & -e_1 \\ e_3 & -e_2 & e_1 & e_0 \end{pmatrix} \begin{pmatrix} 0 \\ \omega'_x \\ \omega'_y \\ \omega'_z \end{pmatrix} \quad (26)$$

The particle translational and rotational equations of motion (eq. (5) and (16)) are solved by a mixed differencing procedure (Fan and Ahmadi (1995)). Equation (10) and equation (26) are solved by a second order Adams Bashforth scheme. Since the constraint (4) should be preserved in time, the Euler parameters are re-scaled after every timestep in order to avoid accumulation of numerical errors (Allan and Tildesley (1987)). The timestep used in the particle equations is the same as that used for the Navier-Stokes equations. The particle boundary conditions are periodic in the two homogeneous directions. If a particle hits the wall, it is re-introduced randomly into the computational domain.

RESULTS AND DISCUSSION

In the present study, six different particle sets are investigated, see table 1. In all cases, the number of particles N is kept constant. The density ratio D is varied in order to fix the response times for different aspect ratios. The results will focus on the orientation of the ellipsoids, where the orientation is described by the three angles (or direction

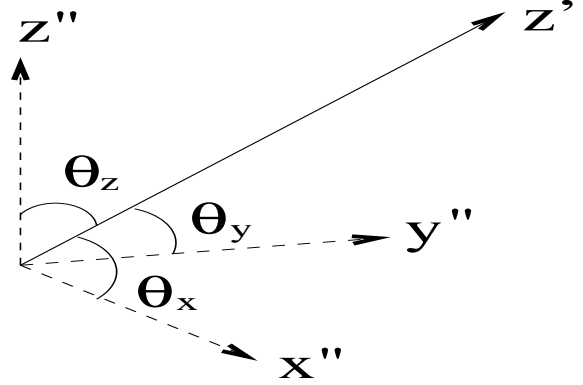


Figure 3: Orientational angles of an ellipsoid with semi-major axis z' .

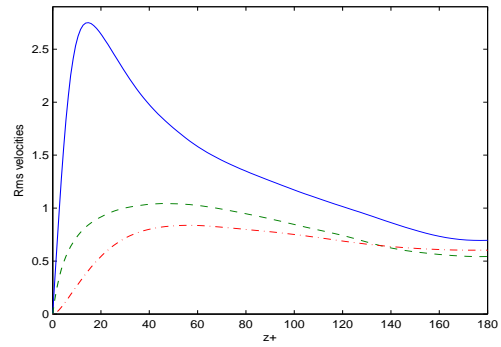


Figure 4: Turbulent velocity fluctuations; (—) Streamwise fluctuations, (- -) spanwise fluctuations, (-.-) wall-normal fluctuations.

cosines) the ellipsoids semi-major axis makes with the axes of the co-moving system, see figure 3.

Figure 4 shows the rms values of the turbulent velocity fluctuations. Even though the channel geometry is relatively small, the characteristic behavior of the second order moments are captured (see also Jimenez and Moin (1993)). It is expected that the turbulent fluctuations will contribute to the orientation of the ellipsoids.

Ellipsoids with equivalent response time $\tau^+ = 0.5$

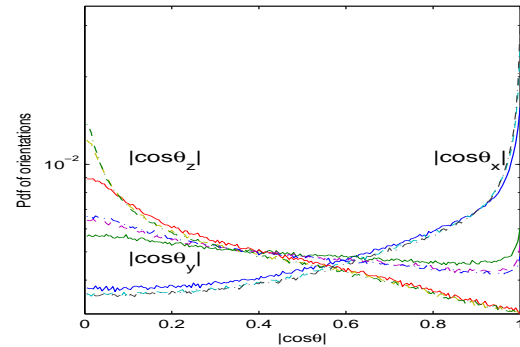


Figure 5: Pdf of particle orientations; (—) Case F10, (- -) Case F30, (-.-) Case F50.

The probability density function of particle orientations (mean direction cosines) is shown in figure 5. It is seen that the particles have large probability of orientation in the

streamwise direction and lower probability of being oriented in the spanwise and wall-normal direction. These probabilities become more pronounced with increased aspect ratio λ .

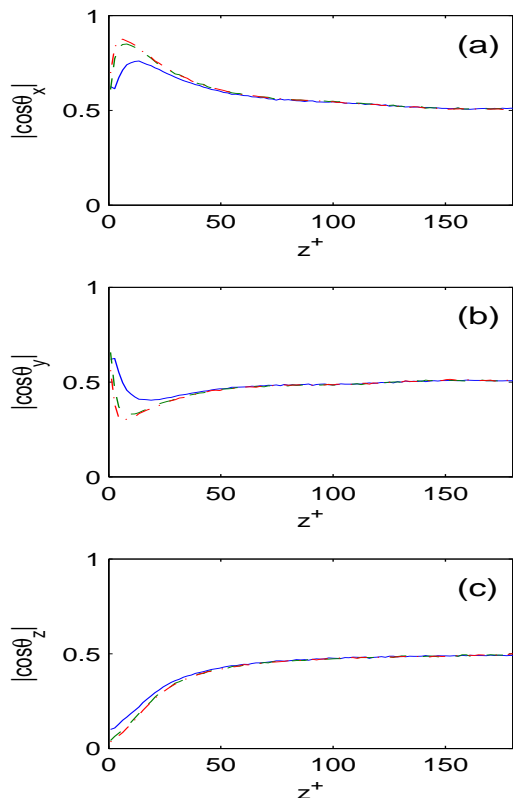


Figure 6: Absolute value of mean direction cosines for ellipsoids with equivalent response time $\tau^+ = 0.5$; (---) Case F10, (-·-) Case F30, (-·-·) Case F50. a) $|\cos\theta_x|$, b) $|\cos\theta_y|$, c) $|\cos\theta_z|$

Figure 6 shows the mean orientations of the ellipsoids relative to x , y and z directions, respectively. It is seen that particles achieve increasing orientation in the streamwise direction in the near-wall region with increasing aspect ratio. Also, it is noted that the peak is shifted towards the wall with increasing aspect ratio. The opposite trend is seen for the spanwise orientation (fig 6b), in which direction the particles seem to be less oriented with increasing aspect ratio. The wall-normal orientation is shown in figure 6c. In the core of the channel, the particles are oriented towards the wall while they are more aligned with the wall in the near-wall region. In the near-wall boundary layer, the streamwise turbulent fluctuations dominate the spanwise and wall-normal fluctuations, see figure 4. It is possible that the net effect of the fluctuations is to stabilize the ellipsoids such that they mostly orient in the streamwise direction due to the dominating streamwise turbulent intensity. Also, since the particles mainly rotate about the y'' axis (not shown here), they will spend most of their time oriented in the streamwise direction. When the aspect ratio increases, the moment of inertia about the two semi-minor axes becomes larger. Hence, the effect is that the ellipsoids have larger probability of being oriented in the streamwise direction with increas-

ing aspect ratio. In the core region of the channel, where the turbulent fluctuations are nearly isotropic, the orientation also becomes isotropic. The particles do not seem to preferentially orient in a specific direction.

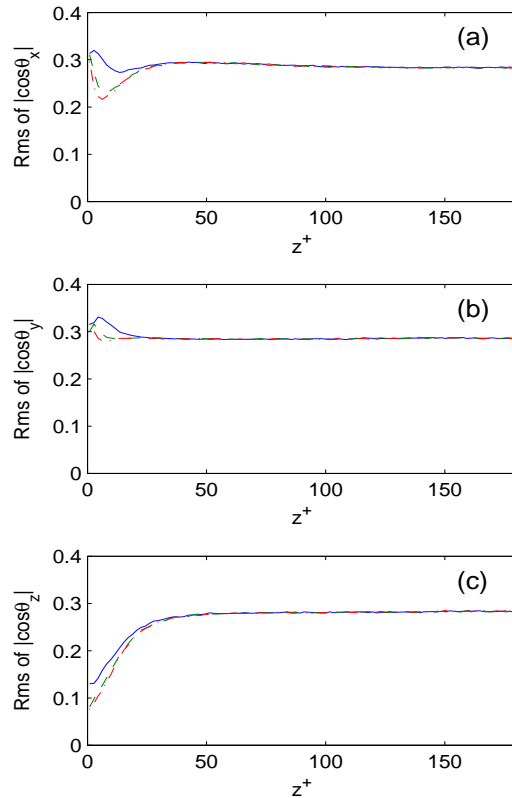


Figure 7: Rms of the direction cosines for ellipsoids with equivalent response time $\tau^+ = 0.5$; (-) Case F10, (-·-) Case F30, (-·-·) Case F50. a) $|\cos\theta_x|$, b) $|\cos\theta_y|$, c) $|\cos\theta_z|$

The fluctuations of the particle orientations are shown in figure 7. Away from the wall the fluctuations become isotropic. In the near-wall region, the orientational fluctuations dominate in streamwise and spanwise directions while they are less prominent in the wall-normal directions.

Ellipsoids with equivalent response time $\tau^+ = 10$

Figure 8 shows the probability of orientation for ellipsoids with equivalent response time $\tau^+ = 10$. Also here it is seen that the particles have larger probability of orienting in the streamwise direction and this tendency increases with aspect ratio. It is interesting to see that case S10 particles behave quite differently than S30 and S50 particles. Comparing case F10 and case S10 it is seen that S10 particles have larger probability of being oriented in the spanwise direction. Also, S10 particles seem to be less oriented in the wall-normal direction, which is also the case for S50 particles.

The absolute value of the mean direction cosines for ellipsoids with equivalent response time $\tau^+ = 10$ is shown in figure 9. Comparing with figure 6, the effect of particle inertia is important for the orientations. In this case, also here the particles seem to preferentially orient in the streamwise direction in the near-wall region. This tendency increases with particle aspect ratio. On the other hand, the particles

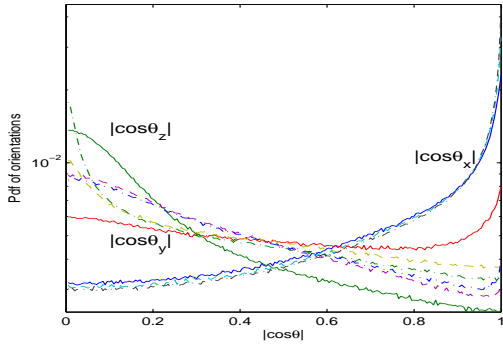


Figure 8: Pdf of particle orientations; (—) Case S10, (---) Case S30, (-·-) Case S50.

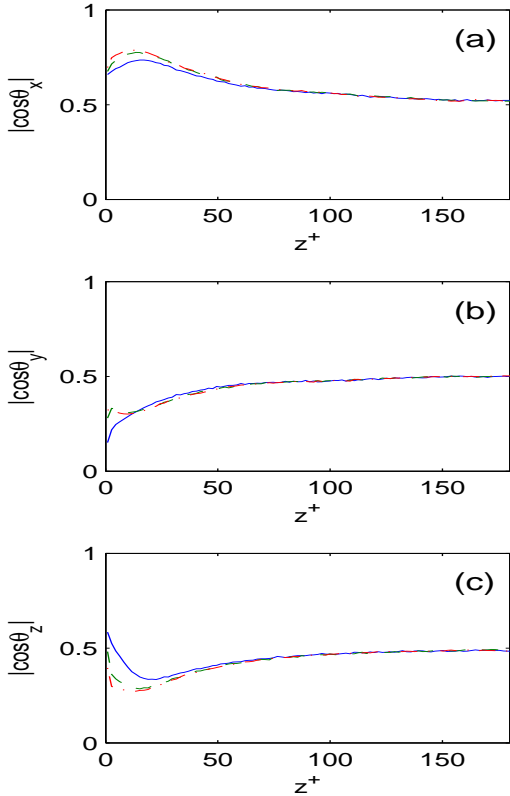


Figure 9: Absolute value of mean direction cosines for ellipsoids with equivalent response time $\tau^+ = 10$; (—) Case S10, (---) Case S30, (-·-) Case S50. a) $|\cos\theta_x|$, b) $|\cos\theta_y|$, c) $|\cos\theta_z|$

seem to be less oriented in the spanwise direction as compared to figure 6 and less aligned with the wall. It is possible that, due to the increased inertia, the particle orientation is basically affected by the mean shear and the dominating streamwise turbulent intensity. The effect of the streamwise turbulent fluctuations would be to orient the particles with the mean flow direction, and the mean shear would rotate the particle about the spanwise axis. Since it is expected that the turbulent intensities contribute more to the orientation for lighter particles (case F10, F30, F50), it can explain why

the rotational motion for heavier particles (case S10, S30, S50) seem to be more confined to the xz -plane with rotation about the spanwise axis. Therefore, the heavier particles will be less oriented in the spanwise direction.

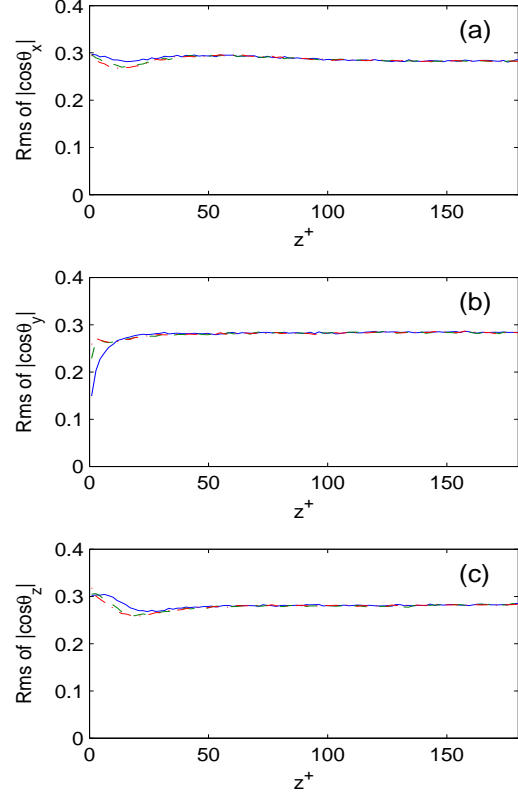


Figure 10: Rms of the direction cosines for ellipsoids with equivalent response time $\tau^+ = 10$; (—) Case S10, (---) Case S30, (-·-) Case S50. a) $|\cos\theta_x|$, b) $|\cos\theta_y|$, c) $|\cos\theta_z|$

Figure 10 shows the fluctuations in orientation for $\tau^+ = 10$ particles. Also here, the fluctuations become more or less isotropic away from the near-wall region ($z^+ > 40$). It is seen that the heavier particles fluctuate more in streamwise and wall-normal orientation. There is a small exception for S10 particles in the region $z^+ < 7$ where the fluctuations in the streamwise orientation for F10 particles are larger. Anyway, the small fluctuations in spanwise orientation support the idea that the rotation of heavier particles is largely confined to the xz -plane.

CONCLUSIONS

Direct numerical simulation has been conducted in order to study the orientation of ellipsoidal particles in a turbulent channel flow. It was assumed that the particles were smaller than the Kolmogorov scales at a frictional Reynolds number of 360. The creeping flow versions of the drag force and torque were applied in the particle equations of motion. Six different particle cases were studied with varying aspect ratios and particle equivalent response times. Results show that, in the near-wall region, prolate ellipsoids tend to orient in the mean flow direction. This effect becomes more pronounced with increasing aspect ratio. The effect of increasing particle inertia causes the rotational motion to be

more confined to the xz -plane, and heavier particles are less oriented in the spanwise direction. In the core region of the channel, the orientations become isotropic.

AKNOWLEDGEMENTS

This work has been supported by The Research Council of Norway through the PETROMAKS programme. The authors would like to thank Professor Goodarz Ahmadi for helpful discussions.

REFERENCES

- Allan, M. P. and Tildesley, D. J., 1987, "Computer Simulation of Liquids," *Oxford University Press*.
- Brenner, H., 1963, "The Stokes resistance on an arbitrary particle", *Chem. Eng. Sci.*, vol. 18, pp. 1-25.
- Brenner, H., 1964, "The Stokes resistance of an arbitrary particle-IV, Arbitrary fields of flow," *Chem. Eng. Sci.*, vol. 19, pp. 703-727.
- Fan, F. G. and Ahmadi, G., 1995, "A sublayer model for wall-deposition of ellipsoidal particles in turbulent streams," *J. Aerosol Sci.*, vol. 26, pp. 813-840.
- Gallily, I., Cohen, A. H., 1979, "On the orderly nature of the motion of nonspherical aerosol particles. II. Inertial collision between a spherical large droplet and axially symmetrical elongated particle," *J. Colloid Interface Sci.*, vol. 68, pp. 338-356.
- Gillissen, J. J. J., Boersma, B. J., Mortensen, P. H. and Andersson, H. I., 2007, "On the performance of the moment approximation for the numerical computation of fiber stress in turbulent channel flow," *Phys. Fluids*, vol. 19, 035102.
- Goldstein, H., 1980, "Classical Mechanics, 2nd Ed.," *Addison-Wesley Publishing Company*.
- Harper, E. Y., and Chang, I. D., 1968, "Maximum dissipation resulting from lift in a slow viscous shear layer", *J. Fluid Mech.*, vol. 33, pp. 209-225.
- Jeffery, G. B., 1922, "The motion of ellipsoidal particles immersed in a viscous fluid," *Proc. R. Soc.*, vol. 102, pp. 161-179.
- Jimenez, J. and Moin, P., 1993, "The minimal flow unit in near-wall turbulence," *J. Fluid Mech.*, vol. 225, pp. 213-240.
- Kuerten, J. G. M., 2006, "Subgrid modeling in particle-laden channel flow," *Phys. Fluids*, vol. 10, pp. 025108.
- Kulick, J.D., Fessler, J.R. and Eaton, J. K., 1994, "Particle response and turbulence modification in fully developed channel flow," *J. Fluid Mech.*, vol. 227, pp. 109-134.
- Lin, J., Shi, X. and Yu, Z., 2003, "The motion of fibers in an evolving mixing layer," *Int. J. Multiphase Flow*, vol. 29, pp. 1355-1372.
- Marchioli, C., Picciotto, M. and Soldati, A., 2007, "Influence of gravity and lift on particle velocity statistics and transfer rates in turbulent vertical channel flow," *Int. J. Multiphase Flow*, vol. 33, pp. 227-251.
- Parsheh, M., Brown, M. L. and Aidun, C. K., 2005, "On the orientation of stiff fibres suspended in turbulent flow in a planar contraction," *J. Fluid Mech.*, vol. 545, pp. 245-269.
- Shapiro, M. and Goldenberg, M., 1993, "Deposition of glass fiber particles from turbulent air flow in a pipe," *J. Aerosol Sci.*, vol 24, pp. 65-87.
- Zhang, H., Ahmadi, G., Fan, F-G. and McLaughlin, J.B., 2001, "Ellipsoidal particles transport and deposition in turbulent channel flows" *Int. J. Multiphase Flow*, vol. 27, pp. 971-1009.